

**OXIDE MINERALS IN COMET WILD 2: TEM AND SYNCHROTRON CHARACTERISATION.** J. C. Bridges<sup>1</sup>, H. C. Changela<sup>1</sup>, J. D. Carpenter<sup>2</sup> and S. J. Gurman<sup>3</sup> Space Research Centre, Dept. of Physics & Astronomy, University of Leicester LE1 7RH, UK [j.bridges@le.ac.uk](mailto:j.bridges@le.ac.uk). <sup>2</sup> ESTEC, Keplerlaan 1, 2201 AZ Noordwijk, The Netherlands. <sup>3</sup> Dept. of Physics & Astronomy, University of Leicester LE1 7RH, UK.

**Introduction:** We have used a variety of techniques – TEM, synchrotron – as part of the UK Stardust consortium in order to identify and constrain the origin of oxides and thus demonstrate some affinities between Wild 2 and other planetary materials such as chondrite groups or IDPs. We are finding that oxidised phases in Wild 2 have a variety of origins. Studying Fe-bearing oxide phases in the Stardust mission Wild 2 samples potentially allows the identification of high temperature phases (e.g. Fe-Cr oxide chromite), space weathering products (nanophase Fe), products of parent body hydrothermal alteration (magnetite), heating and oxidation effects during capture in the aerogel.

**Techniques and Samples:** We have studied a transverse slice from the track 41 keystone (C2044,0,41,0,0), the whole track 134 (C2012,10,134,0,0) and terminal grains from track 121 (C2005,2,121,1,0 and C2005,2,121,2,0). FIB-SEM extraction of Fe oxide-bearing wafers and TEM analyses on track 121 were performed at the University of Leicester using the technique described in [1,2]. Bright field imaging, STEM EDS and Selected Area Electron Diffraction (SAED) were performed on the particle and surrounding gold foil mount. Microfocus XRS, mapping and XANES spectroscopy were performed at Beamline I18 of the Diamond Light Source, Oxfordshire on the track 41 slice, track 134 and mineral standards [1]. This beamline operates from a 3 GeV synchrotron with typical currents of 200 mA. A Si (1 1 1) and (3 1 1) double crystal monochromator was used for energy selection with resolutions of  $10^{-4}$  and  $10^{-5}$  respectively. A 9 element Ge based solid state detector was used which is capable of measuring the X-rays of Ca upwards. Track 41 and track 121 were analysed by microRaman at the University of Kent (C2005,2,121,2,0) [3] and Open University (C2005,2,121,1,0) and that data together with the results of Kent light gas gun experiments designed to ascertain the effects of capture heating are presented in [1]. Track 121 is a ‘carrot’ shaped, 0.9 mm length track, tracks 134 and 41 are type b ‘turnip’ of length 0.38 and 4 mm. The track 41 slice was cut out 0.8 mm from the track entrance.

**Results & Discussion:** Fe  $K\alpha$  X-ray maps taken along track 134 (Fig. 1) show that there is a concentration of Fe-bearing phases towards the terminal end. There are also 2 FeNi grains in the mid track. Fe XANES of the terminal grain of this track (Fig. 2)

shows a very good match to an Fe sulphide standard (pyrrhotite). However the mid track FeNi grains show absorption edges e.g. around 7140 eV which suggest that some oxidation of the metal has occurred during capture. The Track 41 slice contains a range of different minerals and oxidation states (Fig. 3a,b). XRF showed Fe hotspots, Fe-Ni compounds, Fe-Ti (oxide – e.g. ilmenite), Cr-Fe-Mn-Ti-V (oxide-chromite), an unidentified Fe-Zn compound. Fe-XANES analyses show that Fe hotspots have a marked absorption peak at 7110 – 7111 eV, before the main K edge, a peak associated with ferric oxide. Similar effects have been reported elsewhere for ferric oxide-bearing phases [4]. The Fe hotspot patterns are very close to that of the magnetite (absorption peak at 7110 eV) and hematite standards (absorption peak at 7111 eV) and is consistent with a mixture of these 2 phases, a result initially suggested by microRaman analyses [1, 3]. The Fe-Ni grain analysed shows a marked absorbance feature around 7160 eV which distinguishes it from the hematite-magnetite mixes and is consistent with Fe metal [5]. However our sample also has an absorption peak around 7111 eV, which is consistent with a mixture of FeNi metal and ferric oxide. The Fe-Zn compound also shows this absorbance feature showing that it too has been oxidised to some extent, presumably during capture.

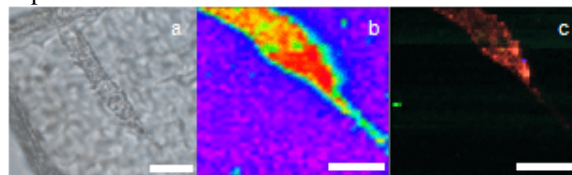


Fig. 1. Synchrotron XRF Maps of Track 134. A. Reflected light (inverted image to b and c). B. Fe  $K\alpha$  map. C. RGB map red Fe  $K\alpha$ , green Ni  $K\alpha$ , blue Ca  $K\alpha$ . Scale bar 50  $\mu\text{m}$ . Each pixel step of 5  $\mu\text{m}$  was integrated with a dwell time of 5 s.

**TEM analysis of Fe oxide in Track 121.** The Fe oxides are revealed as pure Fe and O by TEM-EDS analysis (Fig. 4). Electron diffraction (and microRaman [1]) show the grains in sample C2005,2,121,1,0 to be amorphous. However microRaman analyses show that grains in sample C2005,2,121,2,0 consist of a magnetite-hematite mixture [1]. Thus the Stardust samples contain a mixture of different oxide types in

close proximity. Other phases in track 121 include Mg-silicate and Fe-sulphide.

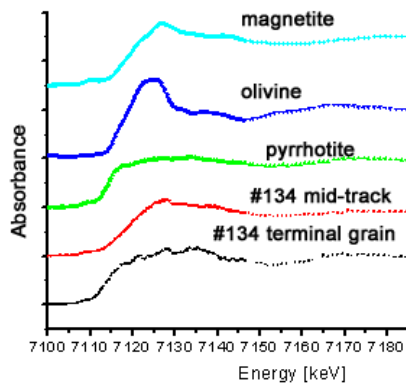


Fig. 2. Fe XANES of Track 134 minerals and standards. The terminal grain has a close fit to FeS pyrrhotite. The mid track FeNi grains show absorbance features similar to magnetite, suggesting that the metal has been partially oxidised during capture in the aerogel.

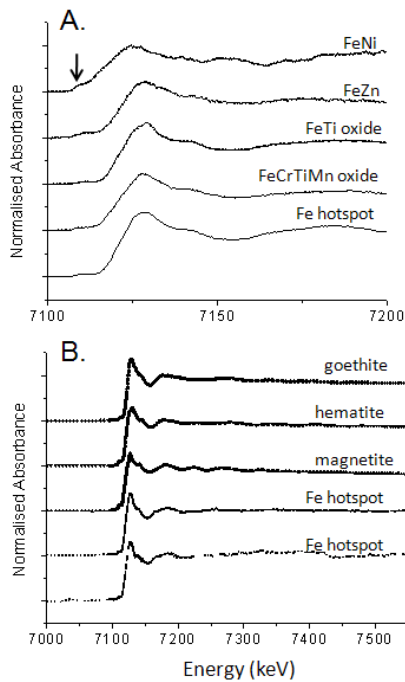


Fig. 3. Synchrotron Fe XANES of Track 41 Minerals and Standards. A. Fe-bearing phases ('hotspots') within track 41. A small absorbance feature around 7110-7112 eV (before the main absorption edges) is arrowed which shows the presence of ferric oxide in all the samples, including the relict FeNi metal and an unidentified Fe-Zn phase. The relict FeNi metal also has an absorbance feature around 7160 eV, a feature characteristic of metal [5]. B. Comparison

between goethite  $\text{FeOOH}$ , hematite  $\text{Fe}_2\text{O}_3$ , magnetite  $\text{Fe}_3\text{O}_4$  standards with Fe hotspots. The main absorption edges have a similar gradient for all the samples and are consistent with the presence of ferric oxide. The closest match to the Fe hotspots is a mixture of magnetite and hematite, consistent with microRaman analyses of the phases reported in [1].

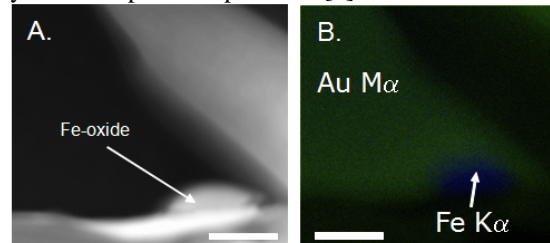


Fig. 4. TEM bright field image (A) and EDS map (B) of amorphous Fe oxide from track 121. The Fe oxide grain showed no electron diffraction (although the Au foil did). Scale bar 0.2  $\mu\text{m}$ .

#### Conclusions - Origin of the Oxide Minerals:

Our results for tracks 41, 121 and 134 are in agreement with the experimental work of [6] who suggested that minerals close to the entrance of 6  $\text{kms}^{-1}$  tracks within aerogel experience some oxidation. This explains oxidation features of relict FeNi metal in tracks 134 and 41. Amorphous Fe oxide in track 121 may also be oxidised Fe metal. The surface of Comet Wild 2 shows space weathering [7] associated with nanophase Fe metal which might be a source of this. The magnetite-hematite, Fe-Ti oxide and chromite are cometary grains. The former might be low temperature, hydrothermal grains whereas the latter are high temperature in origin. Intermixing of reduced and oxidised phases, high and low temperature minerals together with other evidence such as the absence of GEMS [8] are features reminiscent of carbonaceous chondrites.

**Acknowledgments:** The NASA Curatorial Facility prepared track 121 terminal particles. A. Westphal and C. Snead of U. of California (Berkeley) are prepared tracks 41, 134. Synchrotron work was carried out with the support of the Diamond Light Source. The NHM is thanked for mineral standards.

**References:** [1] Bridges J. C. et al. (2009) *Meteorit. Planet. Sci.*, (subm.). [2] Changela H. C. and Bridges J. C. (2009) *LPS XXXX*. [3] Burchell M. J., et al. (2006). *Meteorit. Planet. Sci.* 41, 217 – 232. [4] Prietzel J. et al. (2007) *European J. of Soil Science* 58, 1027-1041. [5] Pingitore N. E. et al. (2002) *Microchemical Journal*, 71, 205-210. [6] Grossemey F. et al. (2008). *J. Planetary and Space Science*, 55, 966-973. [7] Farnham T. L. and Schleicher D. G. (2005) *Icarus* 173, 533-558. [8] Ishii H. A. et al. (2008) *Science*, 319, 447-450.